7-1-1975

MODE Tides

Bernard Zetler

Walter Munk

Wendell Brown

Florence Dormer

Harold Mofjeld

MODE Tides[1]

Bernard Zetler,[2] Walter Munk,[2] Harold Mofjeld,[3] Wendell Brown[2] and Florence Dormer[2]

(Manuscript received 6 October 1974, in revised form 14 January 1975)

ABSTRACT

IGPP and AOML bottom pressure measurements at four MODE stations constitute a unique set of deep-sea tidal measurements (although deployed for other purposes). A response analysis relative to a Bermuda reference has been optimized with regard to the number of complex weights and the makeup of gravitational and radiational inputs. Duplicate instrumentation on EDIE capsule gave 32.067, 2.5°; 32.074, 2.6° for M_2 amplitude (cm) and Greenwich epoch, thus attesting the reality of measured small station *differences* (order 1 cm, 1°). M_2 tidal currents (calculated from the M_2 surface and bottom slopes) have u and v speeds of 0.5 and 0.8 cm s^{-1}, respectively, in rough agreement (both amplitude and phase) with preliminary estimates from current measurements. M_2 and K_1 tides are in accord with some existing cotidal and co-range charts. M_3 tides are a fraction of equilibrium magnitude, whereas M_4, M_5 and M_6 (typically 0.07, 0.05, 0.03 cm) vastly exceed equilibrium values. Presumably these overtides are generated by nonlinear coupling in the world's shallow basins, from where they radiate into the global oceans to attain a level where radiative and dissipative processes are somehow balanced.

1. Introduction

Measurements of bottom pressure during the MODE (Mid-Ocean Dynamics Experiment) experiment, March to July 1973, were for the purpose of studying mesoscale eddies, and accordingly the emphasis was on periods longer and length scales much shorter than those typical of tides. In fact, one premise underlying the experiment was that the "tidal noise" could be effectively eliminated from the records (Brown *et al.*, 1975). In accomplishing this mission, we have performed a unique experiment of simultaneous deep-sea tide measurements. Information concerning instrumentation and experimental procedures has been described separately (Snodgrass *et al.*, 1975).

2. Bermuda reference

The response method (Munk and Cartwright, 1966) was used, following the procedure by Cartwright *et al.* (1969) for the analysis of relatively short deep-sea records. This involves a two-step analysis: (i) the transfer functions of a reference station relative to the tidal potential, and (ii) the transfer functions of the deep-sea records relative to the reference station.

The 1950–60 tide record at Bermuda was used to derive the transfer functions relative to the input potentials; these transfer functions subsequently served as a basis of a Bermuda tide prediction for the MODE period. Table A (Appendix) shows the results[4] of a combined analysis of three 355-day series equally spaced in a period of lunar perigee (8.85 Julian years).

3. MODE transfer functions

Transfer functions and harmonic constants for the seven deep-sea data series[5] are given in Tables B to H. Table 1 is a summary of principal constituents for the five series exceeding one month (thus excluding MERT and EDIE-MARCH). The transfer functions are based on two complex weights (0, −2 days) for diurnal constituents, and three complex weights (0, ±2 days) for semidiurnal constituents (see below). "Grav+rad" and "grav only" refer to separate analyses with regard to the nongravitational (radiational) solar effects; we

[1] MODE Contribution No. 16.

[2] Institute of Geophysics and Planetary Physics, Scripps Institution of Oceanography, University of California, La Jolla 92037.

[3] Atlantic Oceanographic and Meteorological Laboratories, NOAA, Miami, Fla. 33149.

[4] After all of the MODE tide analyses were completed, a small error was found in the analysis of the diurnal tides at Bermuda. Inasmuch as the variation was used consistently in arriving at both the Bermuda harmonic constants and the Bermuda prediction for the MODE period, the accuracy of the MODE tide analyses is not affected. For the record, Table A values and corrected values (in parentheses) are as follows:

	H (cm)	G (deg)
Q_1:	1.13 (1.13)	188.2 (186.6)
O_1:	5.30 (5.30)	192.0 (192.1)
P_1:	2.02 (2.01)	187.7 (187.8)
K_1:	6.56 (6.55)	187.1 (187.0)

[5] IGPP (Institute of Geophysics and Planetary Physics, University of California, San Diego) sea-floor pressure series are named REIKO-MAY, MERT, EDIE-MARCH, EDIE-MAY P1, and EDIE-MAY P2. AOML (Atlantic Oceanographic and Meteorological Laboratories, Miami, Fla.) series are named AOML1 and AOML3.

TABLE 1. Admittances and tidal constants: R is amplitude ratio, ϕ station lead (deg) relative to Bermuda, H amplitude (cm), and G Greenwich epoch (deg). The frequency (cycles per day) is given at the head of each column.

		Grav+rad					Grav only	
		O_1 0.930	K_1 1.003	(N_2) 1.895	M_2 1.932	(S_2) 2.000	M_2 1.932	(S_2) 2.000
	AOML3	1.142	1.138	0.956	0.943	0.877	0.943	0.752
	AOML1	1.156	1.180	0.983	0.967	0.877	0.967	0.764
R	REIKO	1.174	1.187	1.003	0.970	0.838	0.969	0.706
	EDIE-MAY P1	1.172	1.196	0.921	0.9000	0.787	0.900	0.666
	EDIE-MAY P2	1.180	1.184	0.920	0.9002	0.782	0.900	0.663
	AOML3	−4.9	−6.8	0.2	−0.6	− 7.3	−0.6	− 9.1
	AOML1	−5.6	−7.6	−2.1	−2.3	− 6.6	−2.3	− 8.2
ϕ	REIKO	−4.0	−7.4	−1.4	−2.4	− 8.5	−2.4	−12.6
	EDIE-MAY P1	−7.9	−10.3	−3.8	−4.2	−10.3	−4.1	−13.5
	EDIE-MAY P2	−8.0	−10.2	−4.0	−4.3	−10.1	−4.3	−13.3
	AOML3	6.05	7.47	7.82	33.60	7.09	33.60	6.08
	AOML1	6.13	7.74	8.04	34.45	7.08	34.45	6.17
H	REIKO	6.22	7.79	8.20	34.57	6.77	34.53	5.70
	EDIE-MAY P1	6.21	7.84	7.54	32.067	6.35	32.07	5.38
	EDIE-MAY P2	6.25	7.77	7.53	32.074	6.32	32.07	5.36
	AOML3	196.9	193.9	337.5	358.9	31.5	358.9	33.3
	AOML1	197.6	194.7	339.8	0.6	30.8	0.6	32.4
G	REIKO	196.0	194.5	339.1	0.7	32.7	0.7	36.8
	EDIE-MAY P1	199.9	197.4	341.5	2.5	34.5	2.4	37.7
	EDIE-MAY P2	200.0	197.3	341.7	2.6	34.3	2.6	37.5

prefer the grav+rad values. In the past, the choice of the number of weights and the treatment of radiational tides have been subjective. On the basis of MODE and other recent measurements, Zetler and Munk (1975) have established some criteria. Here we shall give a brief review of how the selection was made.

a. Weights

In the response analysis, the measured series is approximated (in the least-square sense) as a weighted sum of the reference series for various leads or lags. For example, a single complex weight $(1+0i)$ for zero lag corresponds to identical series; $0+2i$ corresponds to a measured series in quadrature with the reference series and of twice its amplitude. The vertical lines (solid and dashed) in the bottom left corner of Fig. 1 show a diurnal amplitude ratio of 1.18 and phase lag of 8° of EDIE-MAY P1 relative to Bermuda, obtained for a single (complex) weight.

Munk and Cartwright (1966) recommend lag intervals of 2 days. For two complex weights (lags 0, 2 days) the admittance is now a smoothly varying function of frequency: e.g., the amplitude ratio and phase lag are somewhat larger at higher frequency for the diurnals (see also O_1 and K_1 in Table 1). For additional weights, the admittances become increasingly more wiggly, in part (one surmises) as a result of the noise content. The trick is to terminate when one's credo on the smoothness of oceanic admittances is violated.

To obtain objective criteria, the series was divided into sections A and B. The top left panel gives the variance in the residual of section A predicted from an analysis of A and B, respectively. For self-prediction (A residuals from A weights) one expects, and finds, that the residuals diminish with increasing number of weights. However, after three weights, the improvement is slow and one suspects that the analysis is responding more to noise than to signal. At approximately that point one expects, and finds, that A residuals from B weights should deteriorate. The results are similar for B residuals, except that the overall residual is lower. On this basis the decision was made to stop at two weights. For the semidiurnal tides the "turning point" is a bit later, hence the decision to stop at three weights. The decisions are in general accord with the wiggliness of the admittances, taking into account also the resemblance between admittances from A and B residuals.

b. Radiational tides

Radiational tides are periodic variations in sea level primarily related to meteorological changes such as the semi-daily cycle in barometric pressure and daily land and sea breezes. These cyclical variations match the frequencies of solar (not lunar) gravitational tidal constituents. Cartwright (1966) and Zetler (1971) found the average ratio of radiational amplitude to gravitational amplitude at the S_2 frequency to be about 0.17.

The bandwidths of the radiational tides are much narrower than those of the gravitational tides, essentially covering tidal lines separated by cycles per year (cpy) rather than cycles per month (cpm). Furthermore, the relative amplitudes within the 1 cpm range are quite different for gravitational and radiational tides. In particular, equilibrium K_2/S_2 (grav) is 0.27, whereas the rad ratio is 0.09. A response analysis for a sufficiently long record (as the 10-year Bermuda record) satisfactorily resolves these different bandwidths and amplitude relationships, and the gravitational admittances across tidal bands are expected to be smooth. Inasmuch as traditional tidal analysis for any length of series and response analysis for short series cannot distinguish between gravitational and radiational contributions to a constituent, but instead solve for their vectorial sum, discontinuities in admittances at the S_2 frequency are inevitable. In fact, Zetler (1971) used these discontinuities as a simple means of calculating the radiational S_2 from harmonic constants computed by traditional analysis.

Gravitational and radiational weights were resolved[6] for the Bermuda record and separate gravitational and radiational predictions were prepared for the MODE period. Given these reference predictions for Bermuda, there are three options for analyzing the MODE data: (i) compute gravitational and radiational admittances separately in a combined analysis; (ii) use the gravitational predictions only; and (iii) sum the gravitational and radiational predictions for each species and use the summed complex predicted series as reference.

All three methods were tried. For the first case, it quickly became evident that a much longer deep-sea series was required (probably 10 years) to separate gravitational and radiational contributions. An unstable matrix in solving for the weights resulted in some absurd results (such as a predominance of radiational tides). An extrapolation was made from the (lunar) N_2 and M_2 frequencies to the (solar) S_2 frequency to determine the extent of the discontinuity at the latter frequency, using both the second and third options with EDIE-MAY P1 (Table 1):

	N_2	M_2	S_2		
Frequency (cpd)	1.895	1.932	2.000		
			Extrapolated	Grav +rad	Grav only
R	0.92	0.90	0.86	0.79	0.67
ϕ	−3.8°	−4.2°	−4.9°	−10.3°	−13.5°

[6] Only the gravitational admittances are listed in Table A. The gravitational and radiational constants and their sums are as follows:

	Gravitational		Radiational		Sum	
	H (cm)	G (deg)	H (cm)	G (deg)	H (cm)	G (deg)
P_1	2.16	187.7	0.15	5.9	2.01	187.8
K_1	6.70	187.0	0.15	5.9	6.55	187.0
S_2	9.26	21.7	1.24	185.3	8.08	24.2
K_2	2.31	21.9	0.11	185.3	2.21	22.7

In a comparison of the Bermuda harmonic constants with those obtained for a different period by traditional harmonic analysis (IHB Spec. Publ. No. 26, Sheet 600), the discrepancies in amplitude are less than 4%, in epoch less than 2°.

TABLE 2. Ratio of residual to recorded variance.

	Station				
	AOML3	AOML1	REIKO	EDIE-MAY P1	EDIE-MAY P2
Total (0 to 12 cpd)					
grav+rad	0.00931	0.01338	0.00483	0.00680	0.00948
grav only	0.00937	0.01340	0.00485	0.00680	0.00949
Diurnal (1 cpd$\pm 4\frac{1}{2}$ cpm)					
grav+rad	0.00207	0.00212	0.00051	0.00107	0.00135
grav only	0.00206	0.00192	0.00054	0.00105	0.00136
Semi diurnal (2 cpd$\pm 4\frac{1}{2}$ cpm)					
grav+rad	0.00066	0.00051	0.00014	0.00020	0.00021
grav only	0.00068	0.00056	0.00019	0.00022	0.00024

The discontinuity is smaller for the grav+rad option. Furthermore, residual variances for grav+rad are generally somewhat smaller than for grav only (Table 2). The better results with the grav+rad option indicate a common origin for Bermuda and MODE radiational tides, with a similar relation to the gravitational tides. We would expect the grav only procedure to be superior if Bermuda radiational tides were the result of (i) local effects such as diurnal winds from island heating, or (ii) inverted barometer response to atmospheric pressure (absent from bottom pressure readings). Evidently this is not the case.

c. *Admittance*

Inasmuch as the transducers for EDIE P1 and P2 were only 10 cm apart, a comparison of the two records is a measure of reproducibility of results (Snodgrass *et al.*, 1975). For M_2 the admittances differ by only 2×10^{-4} in amplitude and 0.1° in phase. For the four diurnal tidal constituents listed, the amplitude discrepancy is always less than 1% (the largest being 0.07 cm for K_1) and the phases all agree within 0.1°.

Changes between constituents within each species (relative to Bermuda) are smooth. We find that for O_1 and K_1 relative amplitudes at any one station are within 2%, relative phases within 3°; for N_2 and M_2 the values are 3% and 1°. Yet, the Bermuda reference (Table A) shows marked variation across the semidiurnal band, possibly the result of a free mode. The evidence is for a resonance of large areal extent, rather than highly localized.

The satisfactory agreement at one site assures us of the reality of the small difference between REIKO near the central mooring (28°00′N, 69°40′W) and EDIE-MAY about 150 km to the south-southeast, a small separation when reckoned in tidal dimensions. (The locations of all bottom pressure sensors are shown in Fig. 2). The reasonable fit between the harmonic constants for REIKO and AOML1, roughly 20 km apart near the central mooring, encourages us to discuss jointly results from the IGPP and AOML data. Nevertheless, even though there is no obvious calibration

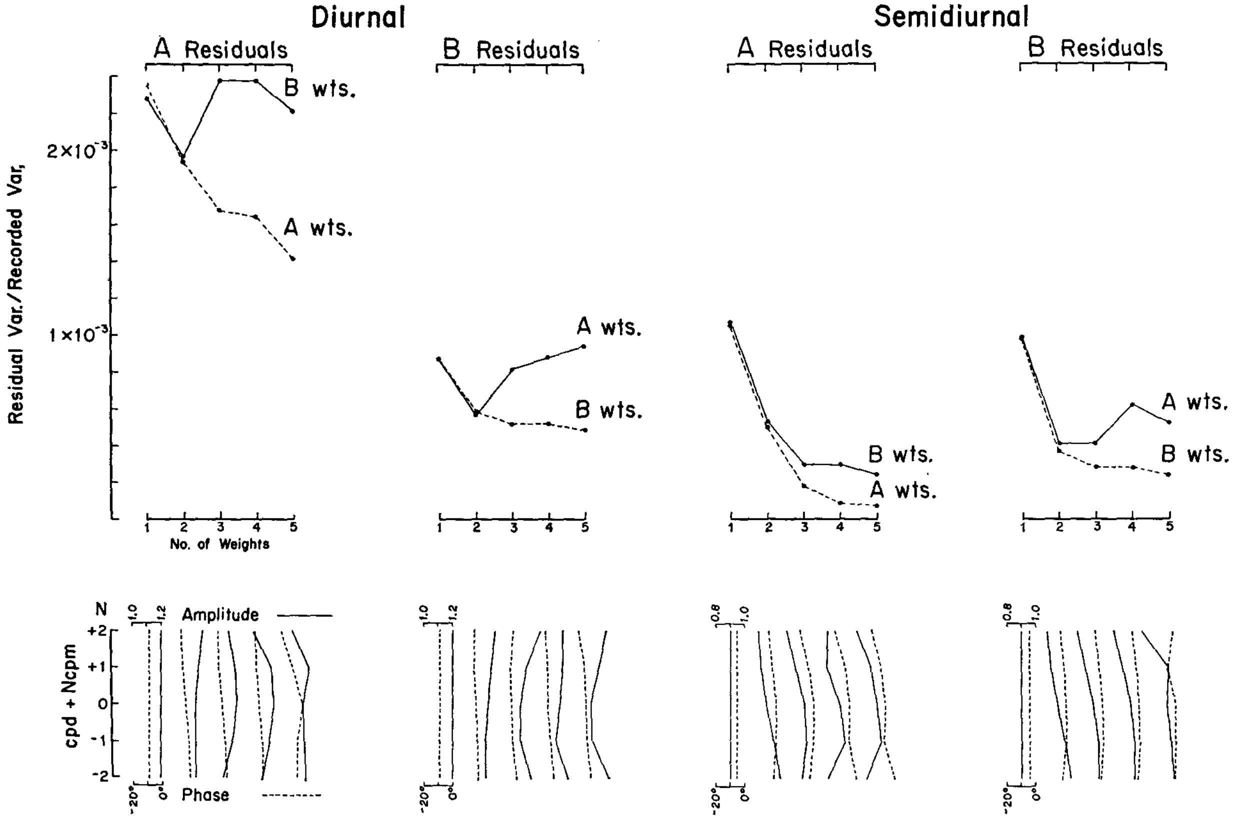

FIG. 1. Analysis of variance for EDIE-MAY P1. The left upper panel gives the ratio of residual to recorded diurnal variance for the first 29 days (record A), with prediction weights based on the A record (self-prediction) and B record (last 29 days), respectively. The remaining upper panel gives the B residuals and corresponding semidiurnal ratios. In each case the dashed lines refer to "self-predictions," the solid lines to future (B residuals from A weights) or past (A residuals from B weights) predictions, respectively. The lower panels give the corresponding amplitude ratios (solid) and phase lags (dashed) relative to Bermuda reference, as a function of frequency (1 cpd±0, 1, 2 cpm for diurnals, 2 cpd±0, 1, 2 cpm for semidiurnals), for 1, 2, . . ., 5 complex weights. With increasing number of weights the self-prediction residuals (but not necessarily those for the future predictions) diminish, and the admittances become increasingly wiggly.

difference between the IGPP and AOML gauges, it seems prudent to use the REIKO, EDIE capsules for comparison between central mooring with the area to the south and the AOML1, AOML3 capsules for comparison between central mooring with the area to the east.

Station differences are consistent for different constituents within each species. At the central mooring the semidiurnal tides are about 8% larger and 2° earlier than at EDIE; the diurnal tides are about equal in amplitude and 3°–4° earlier than at EDIE. Comparing the AOML data, at the central mooring the semidiurnal tides are about 2% larger and 2° later than at AOML3; the diurnal tides slightly smaller and earlier at AOML3. These comparisons imply that both the 1 and 2 cpd tides progress from the northeast, arriving first at AOML3, then the central mooring, and finally at EDIE.

4. Comparison with cotidal charts

There is a general impression that the state-of-the-art in preparing cotidal and co-range charts leaves much to be desired; certainly there are considerable variations between published charts. Most charts deal with only the largest tidal constituent, M_2, sometimes labeling the chart as applying to semidiurnal tides. Similarly, if a chart is designated "diurnal tides," ordinarily it refers to the K_1 constituent. Fig. 2 is a comparison of Dietrich's (1944) charts for M_2 and K_1 with our long series, AOML1 and 3, REIKO, and EDIE-MAY P1 and P2.

a. M_2 tides

Dotted lines show our inference of Dietrich's 0^h15^m and 0^h30^m cotidal lines. All four MODE stations and Bermuda lie between 0^h and 0^h15^m lines (solar hours, not component hours), so their Greenwich epochs should be between 0° and 7.2°. The indicated Bermuda epoch (from our analysis) is 358.3° (IHB sheet 600 gives 0°). Dietrich's 0^h line would need only small displacements to fit the Bermuda values. AOML1, EDIE and REIKO fit Dietrich's chart and are relatively consistent; AOML3 is roughly 3° (6 min in time) early

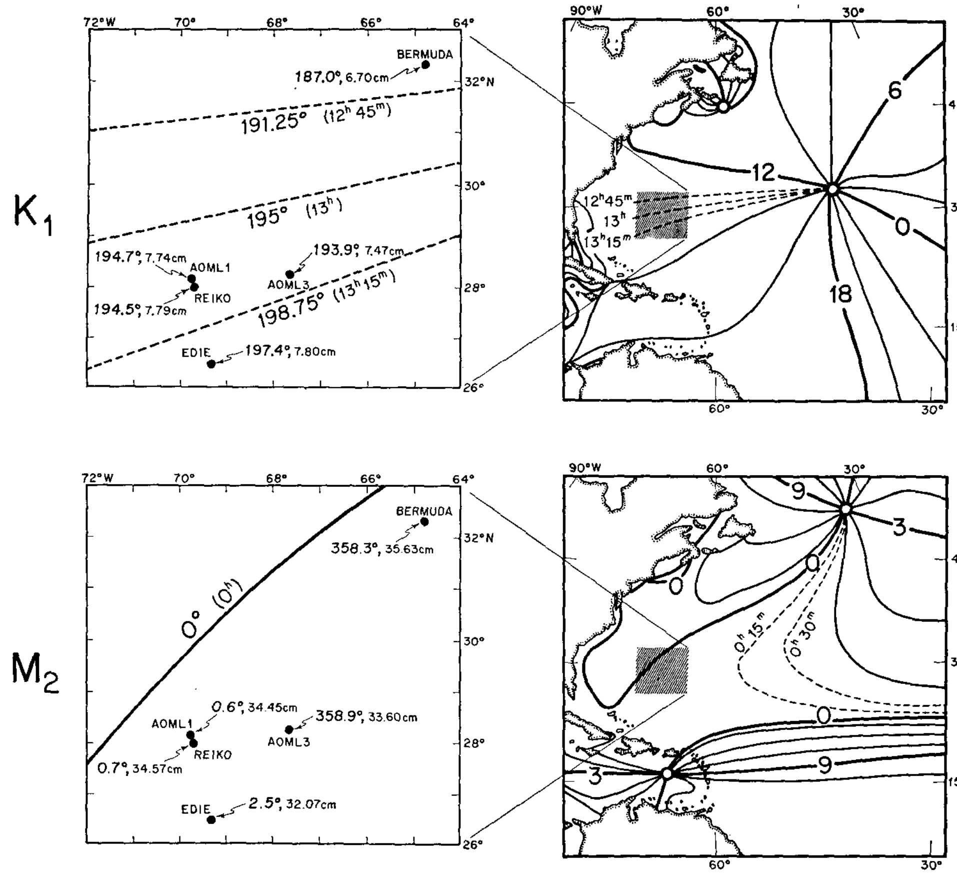

FIG. 2. Right panels show Dietrich's (1944) cotidal lines in the North Atlantic for K_1 and M_2 tides, respectively. Values are in solar hours, with dashed curves designating our interpolation. The MODE area falls within the shaded square which is shown on an enlarged scale in the left panels, for comparison with the results at MODE stations (●).

relative to the other MODE epochs and to the Dietrich configuration. Dietrich does not show co-range lines and the M_2 cotidal lines are too complex in this region to infer readily whether the M_2 amplitudes are consistent with distance from an amphidrome.

Although the Tiron *et al.* (1967) M_2 cotidal chart has the XII^h (same as 0^h) in a similar position and orientation as Dietrich's, one would interpret his progression in time in the MODE area to be to the northwest, contrary to Dietrich's chart and to the values for three MODE stations. The orientation of the Tiron *et al.* XII^h line would call for the AOML3 epoch to be between the epochs of EDIE and the central mooring stations (REIKO and AOML1); thus, on this chart, too, the AOML3 epoch seems to be slightly low (early). The orientation and progression of the Tiron *et al.* co-range lines call for the largest MODE amplitude at the central mooring, as is found to be the case. AOML3 amplitude conforms in that its value falls between those for EDIE and the central mooring.

b. K_1 tides

All stations are roughly 2°–3° early relative to the cotidal lines, yet they are consistent in that they progress toward the south-southeast with spacing matching that of the inferred cotidal lines. As expected, amplitudes increase with distance from the amphidrome.

c. Baroclinic noise

In making detailed comparisons with cotidal charts it should be recognized that the measurements contain a baroclinic contribution of roughly 1% amplitude, $\frac{1}{4}°$ in phase. The characteristic wavelength of the baroclinic tides is 100 km, and at separations of several hundred kilometers the baroclinic contribution to the measured vector sum will differ almost randomly from station to station. This effect exceeds the instrumental noise. If we may assume that barotropic and baroclinic tidal *currents* are of the same order (Section 6), then the pressure *gradients* and associated surface *slopes* are of the same order, 10^{-2} cm km^{-1} for M_2. To obtain baroclinic surface amplitudes we multiply by $\lambda/2\pi$, with $\lambda = 160$ km for the gravest baroclinic mode. This gives a near-bottom baroclinic amplitude of 0.3 cm, and for a random orientation the phase shift is by roughly $\frac{1}{4}°$. If there had been surface measurements, the baroclinic contribution would have been several times larger.

5. Tides of higher order

The high reproducibility of the principal tidal constituents encouraged us to analyze MODE pressures for the relatively small components of higher order. These are derived by the response method, using the equilibrium potential G_3^3 as reference function for M_3, and the nonlinear input functions $G_2^2G_2^2$, $G_2^1G_2^2G_2^2$, $G_2^2G_2^2G_2^2$ (rather than G_4^4, G_5^5, G_6^6) for M_4, M_5, M_6, for the reasons stated below. For comparison, Table 3 includes the principal diurnal and semidiurnal tides, equilibrium amplitudes, and some Bermuda estimates. The amplitudes for the higher-order tides at MODE stations correspond to total species energy and therefore are somewhat higher than comparable values for the specific constituents.

M_3 amplitudes at MODE stations and Bermuda are within a factor of 2, and phases lie within one octant. There is nothing extraordinary about this result other than the satisfaction of detecting a 1 mm constituent in deep-sea records. Amplitudes are somewhat less than the equilibrium value, about the same ratio as for the diurnals.

M_4, M_5, M_6 amplitudes are tiny (typically 0.7, 0.5, 0.3 mm) yet very much *larger* than the equilibrium values (3×10^{-2}, 4×10^{-4}, 3×10^{-6} mm). One's first inclination is to attribute these results to experimental noise. We note that IHB values are generally high, perhaps because they include the noise continuum, whereas other estimates reflect only the coherent signal. AOML3 amplitudes are generally higher. Yet in spite of these inconsistencies we believe the estimates for the higher-order harmonics to be significant, for the reason that phases are not randomly distributed, especially if one allows for the fact that distances between stations are no longer negligible as compared to wavelengths.

There is then the question as to why the M_4, M_5, M_6 amplitudes are so much larger than equilibrium amplitudes. Garrett and Munk (1971) (see also Gallagher and Munk, 1971) have suggested that quadratic and higher-order interactions in the world's shallow basins produce multiple frequencies which leak into the global oceans and attain an equilibrium level for which radiative and dissipative processes are somehow balanced. For these reasons the response method was used with double and triple products of the appropriate semidiurnal and diurnal tide potentials as input functions.

6. Inferred tidal currents

Tidal measurements at two points determine the tidal variations in the average pressure gradient between these points, and impose some conditions on the tidal currents. The tidal displacement of the seafloor (and bottom pressure gauge) must here be taken into account (Munk *et al.*, 1970). We use ξ^S and ξ^B for the radial (upward) displacement, relative to the center of the Earth, of the sea surface and bottom, respectively; $\zeta=\xi^S-\xi^B$ is the surface displacement relative to the sea bottom, as observed.

The gravitational forces of the Moon and Sun are conveniently expressed in terms of the *equilibrium*

TABLE 3. Amplitudes and Greenwich epochs of higher-order tides.

	K_1		M_2		M_3		M_4		M_5		M_6	
	H (cm)	*G* (deg)	*H* (cm)	*G* (deg)	*H* (cm)	*G* (deg)	*H* (cm)	*G* (deg)	*H* (cm)	*G* (deg)	*H* (cm)	*G* (deg)
Equilibrium												
Normalized*	36.9	—	63.2	—	0.76	—	1.1×10^{-2}	—	1.5×10^{-4}	—	1.5×10^{-6}	—
At MODE latitude 28°N	11.8	—	19.0	—	0.22	—	3.0×10^{-3}	—	3.7×10^{-5}	—	3.4×10^{-7}	—
Bermuda												
St. George (IHB p. 600)	6.4	189	35.5	000	0.15	40	0.40	232	—	—	0.18	83
Wunsch (1972)**	—	—	—	—	0.13	74	0.16	260	—	—	—	—
Garrett and Munk (1971)	—	—	36.2	—	—	—	0.18	—	—	—	0.08	—
MODE***												
AOML3	7.5	194	33.6	359	0.078	69	0.134	354	0.58	321	0.031	255
AOML1	7.7	195	34.5	001	0.155	36	0.065	330	0.021	277	0.003	102
REIKO	7.8	195	34.6	001	0.155	38	0.074	278	0.033	262	0.021	125
EDIE-MAY P1	7.8	197	32.1	003	0.136	40	0.077	271	0.050	302	0.032	19
EDIE-MAY P2	7.8	197	32.1	003	0.104	55	0.074	253	0.045	295	0.019	59

* Using the normalization by Munk and Cartwright (1966). K_1, M_2 and M_3 are from Cartwright and Taylor (1971); M_4, M_5 and M_6 are from a computer-generated potential. Latitude factors are

$$(-1)^m\left[\frac{2n+1}{4\pi}\right]^{\frac{1}{2}}\left[\frac{(n-m)!}{(n+m)!}\right]^{\frac{1}{2}} p_n^m\,(\cos\theta)$$

where $\theta=90°-$latitude.

** Some values have been modified in accordance with a recent personal communication.

*** M_3, M_4, M_5 M_6 are derived from total species energy. Epochs for M_4, M_5, M_6 are for the summed tides within the appropriate cpd bands.

TABLE 4. Computed and measured tidal currents.*

	u component		v component	
	Speed (cm s^{-1})	G (deg)	Speed (cm s^{-1})	G (deg)
From pressure gradients [Eq. (4)]	0.49	110	0.80	258
Hendry central mooring				
Measured	0.30	72	0.31	233
Barotropic (0)	0.60	110	0.55	328
Baroclinic (1)	0.37	306	0.64	184
(2)	0.37	218	0.36	108
Hendry average, all depths and moorings	0.49	106	0.38	299

* Values in parentheses are modes obtained by a mode decomposition.

response

$$\left.\begin{aligned}\hat{\zeta}_e^{S}&=(1+k)U/g,\quad \hat{\zeta}_e^{B}=hU/g\\ \zeta_e&=\hat{\zeta}_e^{S}-\hat{\zeta}_e^{B}=(1+k-h)U/g\end{aligned}\right\}\tag{1}$$

of surface, bottom and surface relative to bottom, respectively, and this essentially defines Love numbers k, h (k allows for the self-attraction of the tidal bulge). The procedure does not allow for non-equilibrium self-attraction and loading (Hendershott, 1973).

The equations of motion in the center-of-earth system are

$$\partial_t u-fv=g\partial_x(\hat{\zeta}_e^{S}-\hat{\zeta}^{S}),\quad \partial_t v+fu=g\partial_y(\hat{\zeta}_e^{S}-\hat{\zeta}^{S}),\tag{2}$$

where $f=2\Omega\cos\theta$ is the Coriolis parameter. We now set

$$\hat{\zeta}^{B}=\hat{\zeta}_e^{B},\tag{3}$$

thus assuming that the bottom distortion (unlike the surface) can be adequately represented by the equilibrium configuration. It follows that $\zeta_e^{S}-\hat{\zeta}^{S}=\zeta_e-\zeta$. For harmonic oscillations $\exp(-i\omega t)$, Eqs. (2) can be written in the bottom-of-the-sea system (observation coordinates) as

$$\begin{bmatrix}u\\ v\end{bmatrix}=\frac{g}{f^2-\omega^2}\begin{bmatrix}-i\omega\partial_x+f\partial_y\\ -f\partial_x-i\omega\partial_y\end{bmatrix}(\zeta_e-\zeta).\tag{4}$$

Let the real part of $\zeta_m=A_m\exp -i(\omega t-G_m)$ designate the tidal elevation at station m, and

$$\zeta_{mn}=(A_ne^{iG_n}-A_me^{iG_m})e^{-i\omega t}=A_{mn}e^{iG_{mn}}e^{-i\omega t}$$

the station *difference* between m and n. For M_2, we have the following:

	AOML1	AOML3	ζ_{13}	EDIE	REIKO	ζ_{ER}
A (cm)	34.45	33.60	1.32	32.07	34.57	2.72
G (deg)	0.6	358.9	229.7	2.55	0.7	338.3

The average tidal gradient over the MODE area has been obtained from the station differences according to

$$\left.\begin{aligned}\zeta_{13}&=L_{13}(\partial_x\zeta\cos\phi_{13}+\partial_y\zeta\sin\phi_{13})\\ \zeta_{ER}&=L_{ER}(\partial_x\zeta\cos\phi_{ER}+\partial_y\zeta\sin\phi_{ER})\end{aligned}\right\},\tag{5}$$

with $L_{13}=218$ km, $L_{ER}=171$ km, $\phi_{13}=3°$, $\phi_{ER}=102°$ designating the appropriate station separations and bearings for AOML1 and 3, REIKO and EDIE. The corresponding equilibrium gradients derived from

$$U/g=(24.39\text{ cm})\sin^2\theta\exp[-i(\omega t+2\lambda)]$$

are as follows:

$$\left.\begin{aligned}\partial_x\zeta_e&=R^{-1}(1+k-h)(2\times24.39)\\ &\qquad\times\sin\theta\exp[-i(\omega t+2\lambda+\pi/2)]\\ \partial_y\zeta_e&=R^{-1}(1+k-h)(24.39)\\ &\qquad\times\sin2\theta\exp[-i(\omega t+2\lambda+\pi)]\end{aligned}\right\},\tag{6}$$

where $k=0.29$, $h=0.59$ are the Love numbers, $\theta=62°$ is colatitude, $\lambda=-70°$ is east longitude, and R the equatorial radius of the earth. The numerical values from (5) and (6) are

	$\partial_x\zeta$	$\partial_y\zeta$	$\partial_x\zeta_e$	$\partial_y\zeta_e$
A (cm km^{-1})	0.63×10^{-2}	1.57×10^{-2}	0.47×10^{-2}	0.22×10^{-2}
G (deg)	222.4	333.9	50.0	320.0

M_2 tidal currents were then computed from (4), using $f=6.8\times10^{-5}$ s^{-1}. Listed with them in Table 4 are some analyses of current records by Ross Hendry, MIT: (i) the measured near-bottom currents; (ii) the contributions to near-bottom currents from various modes, using a mode decomposition of current profiles at the central mooring; (iii) an average over all depths and for many moorings.

In principle, the currents computed from (4) are to be interpreted as the *total* tidal current (barotropic plus baroclinic) at the depth of the array. The difficulty is that the spacing between stations (~200 km), though small compared to the barotropic wavelength, is comparable to the baroclinic wavelength ($\lambda=160$ km for mode 1), so that the baroclinic contributions are substantially reduced in an average taken between stations. We may then look for a first-order agreement between the computed values and the barotropic component (whether derived from mode separation or by averaging), and this is roughly what is found. But the baroclinic contributions at a given point are comparable to the barotropic contribution, as has long been known, and for a detailed comparison it would be necessary to resolve the baroclinic cotidal field by closely spaced stations.

Acknowledgments. This work was supported by the Office of Naval Research (Contract N00014-69-A-0200-6008) and the National Science Foundation (Grant NSF-GX-29052). We have received helpful comments by Ross Hendry and Carl Wunsch.

APPENDIX

Results of MODE Tide Measurements

TABLE A.

Station: Bermuda standard tide gauge — 32°24′N, 64°42′W

First series starts 1950 May 21 (441652–450171)†

Second series starts 1953 May 2 (467500–476019)

Combined solution using meaned matrices — Third series starts 1956 April 14 (493372–501891)

Reference: Gravitational and radiational potentials: $G_2^1(0, \pm2, \pm4)$, $G_2^2(0, \pm2, \pm4)$, $G_3^1(0)$, $G_3^2(0)$, $R_1^1(0)$, $R_2^1(0)$, $R_2^2(0)$

Admittances‡ (Station/Reference), Intervals 1 cpm (0.0366011 cpd)

Frequency (cpd)	Real	Imaginary	R	ϕ* (deg)
0.8929346	0.2221	−0.0316	0.2244	−8.1
0.9295357	0.1976	−0.0421	0.2020	−12.0
0.9661368	0.1820	−0.0250	0.1837	−7.8
1.0027379	0.1823	−0.0214	0.1835	−6.7
1.0393390	0.1956	−0.0433	0.2003	−12.5
1.8590714	0.6266	0.3772	0.7314	31.0
1.8956725	0.6259	0.2589	0.6773	22.5
1.9322736	0.5636	0.0169	0.5369	1.7
1.9688747	0.4340	−0.1248	0.4516	−16.0
2.0054758	0.2677	−0.1078	0.2885	−21.9

Principal harmonic constituents

	Frequency (cpd)	Station H (cm)	Station G* (deg)	Reference (gravitational only) H (cm)	Reference (gravitational only) G* (deg)
(Q_1)	0.8932441	1.13	188.2**	5.02	0
O_1	0.9295357	5.30	192.0**	26.22	0
(P_1)	0.9972621	2.02**	187.7	12.21	0
K_1	1.0027379	6.56**	187.1**	36.88	0
(N_2)	1.8959820	8.18	337.7	12.10	0
M_2	1.9322736	35.63	358.3	63.19	0
(S_2)	2.0000000	8.08	24.2	29.40	0
K_2	2.0054758	2.21	22.7	8.00	0

† Greenwich hours since 1900 January 1, 0^h.

‡ Dimensionless.

* G is Greenwich epoch, ϕ is station lead.

** Small corrections for those values listed in the text.

TABLE B.

Station: REIKO-MAY Pressure — 1 June–5 July 1973 — 27°58.2′N, 69°40.4′W

(643496 to 644368 Greenwich hours since 1900 January 1 0^h)

Reference: Bermuda summed complex prediction: $G_2^1+G_3^1+R_1^1+R_2^1$ $(0, -2)$, $G_2^2+G_3^2+R_2^2$ $(0, \pm2)$

Admittances† (Station/Reference), Intervals 1 cpm (0.0366011 cpd)

Frequency (cpd)	Real	Imaginary	R	ϕ* (deg)
0.8929346	1.1459	−0.0560	1.1473	−2.8
0.9295357	1.1713	−0.0823	1.1742	−4.0
0.9661368	1.1824	−0.1172	1.1882	−5.7
1.0027379	1.1768	−0.1533	1.1868	−7.4
1.0393390	1.1558	−0.1832	1.1702	−9.0

Recorded variance: 85.3 cm²
Residual variance: 0.043 cm²
Ratio: 0.00051

Frequency (cpd)	Real	Imaginary	R	ϕ* (deg)
1.8590714	0.9946	−0.0372	0.9953	−2.1
1.8956725	1.0025	−0.0252	1.0028	−1.4
1.9322736	0.9693	−0.0400	0.9702	−2.4
1.9688747	0.9020	−0.0787	0.9055	−5.0
2.0054758	0.8145	−0.1331	0.8253	−9.3

Recorded variance: 674 cm²
Residual variance: 0.098 cm²
Ratio: 0.00014

Principal harmonic constituents

	Frequency (cpd)	Station H (cm)	Station G* (deg)	Reference H (cm)	Reference G* (deg)
(Q_1)	0.8932441	1.30	191.0	1.13	188.2
O_1	0.9295357	6.22	196.0	5.30	192.0
(P_1)	0.9972621	2.40	194.9	2.02	187.7
K_1	1.0027379	7.79	194.5	6.56	187.1
(N_2)	1.8959820	8.20	339.1	8.18	337.7
M_2	1.9322736	34.57	0.7	35.63	358.3
(S_2)	2.0000000	6.77	32.7	8.08	24.2
K_2	2.0054758	1.82	32.0	2.21	22.7

† Dimensionless.

* G is Greenwich epoch, ϕ is station lead.

TABLE C.

Station: MERT-Pressure 17 March–1 April 1973 27°59.3′N, 69°40.3′W
(641741 to 642089 Greenwich hours since 1900 January 1 0^h)
Reference: Bermuda summed complex prediction: $G_2^1+G_3^1+R_1^1+R_2^1$ (0, −2), $G_2^2+G_3^2+R_2^2$ (0, −2)

Admittances† (Station/Reference)					Principal harmonic constituents					
Intervals 1 cpm (0.0366011 cpd)							Station		Reference	
Frequency (cpd)	Real	Imaginary	R	ϕ* (deg)		Frequency (cpd)	H (cm)	G* (deg)	H (cm)	G* (deg)
0.8929346	1.3560	−0.1951	1.3699	−8.2	(Q_1)	0.8932441	1.55	196.4	1.13	188.2
0.9295357	1.2718	−0.2041	1.2881	−9.1	O_1	0.9295357	6.83	201.1	5.30	192.0
0.9661368	1.1924	−0.1747	1.2051	−8.3						
					(P_1)	0.9972621	2.32	193.9	2.02	187.7
1.0027379	1.1342	−0.1132	1.1399	−5.7	K_1	1.0027379	7.48	192.8	6.56	187.1
1.0393390	1.1094	−0.0323	1.1099	−1.7						
Recorded variance: 34.0 cm²										
Residual variance: 0.302 cm²										
Ratio: 0.0089										
1.8590714	0.9496	0.0889	0.9537	5.3						
1.8956725	0.9647	0.0361	0.9654	2.1	(N_2)	1.8959820	7.90	335.6	8.18	337.7
1.9322736	0.9549	−0.0178	0.9550	−1.1	M_2	1.9322736	34.03	359.4	35.63	358.3
1.9688747	0.9221	−0.0618	0.9241	−3.8						
					(S_2)	2.0000000	7.15	29.7	8.08	24.2
2.0054758	0.8732	−0.0867	0.8775	−5.7	K_2	2.0054758	1.94	28.4	2.21	22.7
Recorded variance: 471 cm²										
Residual variance: 0.263 cm²										
Ratio: 0.00056										

† Dimensionless.
* G is Greenwich epoch, ϕ is station lead.

TABLE D.

Station: EDIE-March Pressure 20 March–9 April 1973 26°26.9′N, 69°19.0′W
(641810 to 642282 Greenwich hours since 1900 January 1 0^h)
Reference: Bermuda summed complex prediction: $G_2^1+G_3^1+R_1^1+R_2^1$ (0, −2), $G_2^2+G_3^2+R_2^2$ (0, −2)

Admittances† (Station/Reference)					Principal harmonic constituents					
Intervals 1 cpm (0.0366011 cpd)							Station		Reference	
Frequency (cpd)	Real	Imaginary	R	ϕ* (deg)		Frequency (cpd)	H (cm)	G* (deg)	H (cm)	G* (deg)
0.8929346	1.0705	−0.1095	10.761	−5.8	(Q_1)	0.8932441	1.22	194.0	1.13	188.2
0.9295357	1.1343	−0.1430	1.1433	−7.2	O_1	0.9295357	6.06	199.2	5.30	192.0
0.9661368	1.1766	−0.2014	1.1938	−9.7						
					(P_1)	0.9972621	2.46	200.1	2.02	187.7
1.0027379	1.1886	−0.2724	1.2195	−12.9	K_1	1.0027379	8.00	200.0	6.56	187.1
1.0393390	1.1679	−0.3415	1.2167	−16.3						
Recorded variance: 54.2 cm²										
Residual variance: 0.098 cm²										
Ratio: 0.0018										
1.8590714	0.8566	0.0725	0.8597	4.8						
1.8956725	0.8797	0.0254	0.8800	1.7	(N_2)	1.8959820	7.20	336.1	8.18	337.7
1.9322736	0.8794	−0.0270	0.8798	−1.8	M_2	1.9322736	31.35	0.1	35.63	358.3
1.9688747	0.8559	−0.0738	0.8591	−4.9						
					(S_2)	2.0000000	6.69	31.3	8.08	24.2
2.0054758	0.8140	−0.1054	0.8208	−7.4	K_2	2.0054758	1.81	30.1	2.21	22.7
Recorded variance: 518 cm²										
Residual variance: 0.157 cm²										
Ratio: 0.00030										

† Dimensionless.
* G is Greenwich epoch, ϕ is station lead.

TABLE E.

Station: EDIE-May P1 — 12 May–9 July 1973 — 26°27.8′N, 69°19.6′W
(643072 to 644468 Greenwich hours since 1900 January 1 0^h)
Reference: Bermuda summed complex prediction: $G_2^1+G_3^1+R_1^1+R_2^1$ (0, −2,) $G_2^2+G_3^2+R_2^2$ (0, ±2)

Admittances† (Station/Reference), Intervals 1 cpm (0.0366011 cpd): Frequency (cpd)	Real	Imaginary	R	ϕ* (deg)		Principal harmonic constituents: Frequency (cpd)	Station H (cm)	Station G* (deg)	Reference H (cm)	Reference G* (deg)
0.8929346	1.1378	−0.1465	1.1472	−7.3	(Q_1)	0.8932441	1.30	195.5	1.13	188.2
0.9295357	1.1609	−0.1621	1.1722	−7.9	O_1	0.9295357	6.21	199.9	5.30	192.0
0.9661368	1.1748	−0.1864	1.1894	−9.0						
					(P_1)	0.9972621	2.41	197.8	2.02	187.7
1.0027379	1.1764	−0.2142	1.1957	−10.3	K_1	1.0027379	7.84	197.4	6.56	187.1
1.0393390	1.1654	−0.2399	1.1899	−11.6						

Recorded variance: 76.0 cm²
Residual variance: 0.082 cm²
Ratio: 0.0011

Frequency (cpd)	Real	Imaginary	R	ϕ* (deg)		Frequency (cpd)	Station H (cm)	Station G* (deg)	Reference H (cm)	Reference G* (deg)
1.8590714	0.9013	−0.0845	0.9053	−5.4						
1.8956725	0.9192	−0.0608	0.9213	−3.8	(N_2)	1.8959820	7.54	341.5	8.18	337.7
1.9322736	0.8976	−0.0652	0.9000	−4.2	M_2	1.9322736	32.07	2.5	35.63	358.3
1.9688747	0.8410	−0.0968	0.8465	−6.6						
					(S_2)	2.0000000	6.35	34.5	8.08	24.2
2.0054758	0.7611	−0.1490	0.7755	−11.1	K_2	2.0054758	1.71	33.8	2.21	22.7

Recorded variance: 556 cm²
Residual variance: 0.109 cm²
Ratio: 0.00020

† Dimensionless.
* G is Greenwich epoch, ϕ is station lead.

TABLE F.

Station: EDIE-May P2 — 12 May–9 July 1973 — 26°27.8′N 69°19.6′W
(643072 to 644468 Greenwich hours since 1900 January 1 0^h)
Reference: Bermuda summed complex prediction: $G_2^1+G_3^1+R_1^1+R_2^1$ (0, −2), $G_2^2+G_3^2+R_2^2$ (0, ±2)

Admittances† (Station/Reference), Intervals 1 cpm (0.0366011 cpd): Frequency (cpd)	Real	Imaginary	R	ϕ* (deg)		Principal harmonic constituents: Frequency (cpd)	Station H (cm)	Station G* (deg)	Reference H (cm)	Reference G* (deg)
0.8929346	1.1543	−0.1456	1.1635	−7.2	(Q_1)	0.8932441	1.31	195.4	1.13	188.2
0.9295357	1.1681	−0.1644	1.1796	−8.0	O_1	0.9295357	6.25	200.0	5.30	192.0
0.9661368	1.1721	−0.1872	1.1870	−9.1						
					(P_1)	0.9972621	2.39	197.7	2.02	187.7
1.0027379	1.1656	−0.2095	1.1843	−10.2	K_1	1.0027379	7.77	197.3	6.56	187.1
1.0393390	1.1498	−0.2266	1.1720	−11.1						

Recorded variance: 75.5 cm²
Residual variance: 0.102 cm²
Ratio: 0.0013

Frequency (cpd)	Real	Imaginary	R	ϕ* (deg)		Frequency (cpd)	Station H (cm)	Station G* (deg)	Reference H (cm)	Reference G* (deg)
1.8590714	0.8971	−0.0861	0.9012	−5.5						
1.8956725	0.9182	−0.0638	0.9204	−4.0	(N_2)	1.8959820	7.53	341.7	8.18	337.7
1.9322736	0.8977	−0.0677	0.9002	−4.3	M_2	1.9322736	32.07	2.6	35.63	358.3
1.9688747	0.8399	−0.0969	0.8454	−6.6						
					(S_2)	2.0000000	6.32	34.3	8.08	24.2
2.0054758	0.7568	−0.1454	0.7707	−10.9	K_2	2.0054758	1.70	33.6	2.21	22.7

Recorded variance: 556 cm²
Residual variance: 0.115 cm²
Ratio: 0.00021

† Dimensionless.
* G is Greenwich epoch, ϕ is station lead.

TABLE G.

Station: AOML1 Pressure — 12 March–29 June 1973 — 28°08.4′N, 69°45.2′W
(641593–644225 Greenwich hours since 1900 January 1 0h)
Reference: Bermuda summed complex prediction: $G_2^1+G_3^1+R_1^1+R_2^1$ (0, −2), $G_2^2+G_3^2+R_2^2$ (0, ±2)

Admittances† (Station/Reference), Intervals 1 cpm (0.0366011 cpd): Frequency (cpd)	Real	Imaginary	R	ϕ* (deg)		Principal harmonic constituents: Frequency (cpd)	Station H (cm)	Station G* (deg)	Reference H (cm)	Reference G* (deg)
0.8929346	1.1282	−0.1014	1.1327	−5.1	(Q_1)	0.8932441	1.28	193.3	1.13	188.2
0.9295357	1.1502	−0.1127	1.1557	−5.6	O_1	0.9295357	6.13	197.6	5.30	192.0
0.9661368	1.1650	−0.1326	1.1725	−6.5						
					(P_1)	0.9972621	2.38	195.2	2.02	187.7
1.0027379	1.1693	−0.1569	1.1798	−7.6	K_1	1.0027379	7.74	194.7	6.56	187.1
1.0393390	1.1625	−0.1807	1.1764	−8.8						

Recorded variance: 54.9 cm²
Residual variance: 0.116 cm²
Ratio: 0.0021

Frequency (cpd)	Real	Imaginary	R	ϕ* (deg)		Frequency (cpd)	Station H (cm)	Station G* (deg)	Reference H (cm)	Reference G* (deg)
1.8590714	0.9678	−0.0589	0.9695	−3.5						
1.8956725	0.9824	−0.0366	0.9831	−2.1	(N_2)	1.8959820	8.04	339.8	8.18	337.7
1.9322736	0.9663	−0.0386	0.9670	−2.3	M_2	1.9322736	34.45	0.6	35.63	358.3
1.9688747	0.9228	−0.0645	0.9251	−4.0						
					(S_2)	2.0000000	7.08	30.8	8.08	24.2
2.0054758	0.8610	−0.1088	0.8679	−7.2	K_2	2.0054758	1.92	29.9	2.21	22.7

Recorded variance: 609 cm²
Residual variance: 0.310 cm²
Ratio: 0.00051

† Dimensionless.
* G is Greenwich epoch, ϕ is station lead.

TABLE H.

Station: AOML3 pressure — 11 April–5 July 1973 — 28°14.2′N, 67°32.2′W
(642325–644367 Greenwich hours since 1900 January 1 0h)
Reference: Bermuda summed complex prediction: $G_2^1+G_3^1+R_1^1+R_2^1$ (0, −2), $G_2^2+G_3^2+R_2^2$ (0, ±2)

Admittances† (Station/Reference), Intervals 1 cpm (0.0366011 cpd): Frequency (cpd)	Real	Imaginary	R	ϕ* (deg)		Principal harmonic constituents: Frequency (cpd)	Station H (cm)	Station G* (deg)	Reference H (cm)	Reference G* (deg)
0.8929346	1.1281	−0.0812	1.1310	−4.1	(Q_1)	0.8932441	1.28	192.3	1.13	188.2
0.9295357	1.1372	−0.0980	1.1414	−4.9	O_1	0.9295357	6.05	196.9	5.30	192.0
0.9661368	1.1379	−0.1171	1.1440	−5.9						
					(P_1)	0.9972621	2.30	194.4	2.02	187.7
1.0027379	1.1301	−0.1346	1.1381	−6.8	K_1	1.0027379	7.47	193.9	6.56	187.1
1.0393390	1.1153	−0.1467	1.1250	−7.5						

Recorded variance: 60.2 cm²
Residual variance: 0.125 cm²
Ratio: 0.0021

Frequency (cpd)	Real	Imaginary	R	ϕ* (deg)		Frequency (cpd)	Station H (cm)	Station G* (deg)	Reference H (cm)	Reference G* (deg)
1.8590714	0.9454	−0.0213	0.9457	−1.3						
1.8956725	0.9557	0.0024	0.9557	0.1	(N_2)	1.8959820	7.82	337.5	8.18	337.7
1.9322736	0.9428	−0.0092	0.9429	−0.6	M_2	1.9322736	33.60	358.9	35.63	358.3
1.9688747	0.9095	−0.0540	0.9111	−3.4						
					(S_2)	2.0000000	7.09	31.5	8.08	24.2
2.0054758	0.8626	−0.1225	0.8712	−8.1	K_2	2.0054758	1.93	30.8	2.21	22.7

Recorded variance: 611 cm²
Residual variance: 0.402 cm²
Ratio: 0.00066

† Dimensionless.
* G is Greenwich epoch, ϕ is station lead.

REFERENCES

Brown, W., W. Munk, F. Snodgrass, H. Mofjeld and B. Zetler, 1975: MODE bottom experiment. *J. Phys. Oceanogr.*, **5**, 75–85.

Cartwright, D. E., 1968: A unified analysis of tides and surges round north and east Britain. *Phil. Trans. Roy. Soc. London*, **A263**, 1–55.

——, W. Munk and B. Zetler, 1969: Pelagic tidal measurements. *Trans. Amer. Geophys. Union*, **50**, 472–477.

——, and R. J. Tayler, 1971: New Computations of the tide-generating potential. *Geophys. J. Roy. Astron. Soc.*, **23**, 45–74.

Dietrich, G., 1944: Die Schwingungssysteme der halb-und eintägigen Tiden in den Ozeanen. *Veröffentl. Inst. Meereskunde Univ. Berlin*, **A41**, 7–68.

Gallagher, B. S., and W. H. Munk, 1971: Tides in shallow water: Spectroscopy *Tellus*, **23**, 346–363.

Garrett, C. J. R., and W. H. Munk, 1971: The age of the tide and the "Q" of the oceans. *Deep-Sea Res.*, **18**, 493–503.

Hendershott, M. C., 1973: Ocean tides. *Trans. Amer. Geophys. Union*, **54**, 76–86.

Munk, W. H. and D. E. Cartwright, 1966: Tidal spectroscopy and prediction. *Phil. Trans. Roy. Soc. London*, **A259**, 533–581.

——, F. E. Snodgrass and M. Wimbush, 1970: Tides off shore—Transition from California coastal to deep-sea waters. *Geophys. Fluid Dyn.*, **1**, 161–235.

Snodgrass, F., W. Brown and W. Munk, 1975: MODE: IGPP measurements of bottom pressure and temperature. *J. Phys. Oceanogr.*, **5**, 63–74.

Tiron, K. D., Y. Sergeev and A. Michurin, 1967: Tidal charts for the Pacific, Atlantic and Indian Oceans. *Vestnik Leningrad Univ.*, **24**, 123–135.

Wunsch, C., 1972: Bermuda sea level in relation to tides, weather, and baroclinic fluctuations. *Rev. Geophys. Space Phys.*, **10**, 1–49.

Zetler, B. D., 1971: Radiational ocean tides along the coasts of the United States. *J. Phys. Oceanogr.*, **1**, 34–38.

——, and W. H. Munk, 1975: The optimum wiggliness of tidal admittances. *J. Marine Res.* (in press).